

# Magnetic Control of the Light Reflection Anisotropy in a Biogenic Guanine Microcrystal Platelet

Masakazu Iwasaka,<sup>\*,†,‡</sup> Yuri Mizukawa,<sup>†</sup> and Nicholas W. Roberts<sup>§</sup>

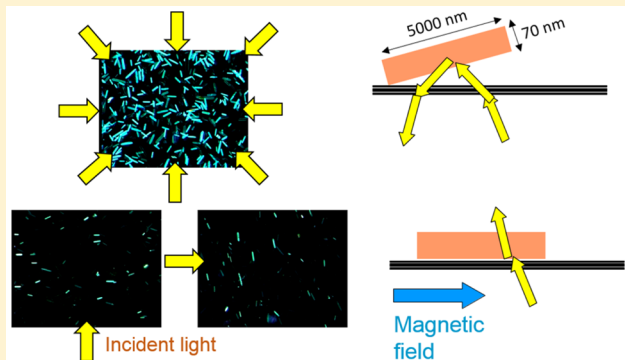
<sup>†</sup>Hiroshima University, 1-4-2 Kagamiyama, Higashi-Hiroshima, 739-8527 Hiroshima, Japan

<sup>‡</sup>Japan Science and Technology Agency, PRESTO, 4-1-8 Honcho, Kawaguchi, 332-0012 Saitama, Japan

<sup>§</sup>School of Biological Sciences, University of Bristol, Tyndall Avenue, Bristol BS8 1TQ, U.K.

## Supporting Information

**ABSTRACT:** Bioinspired but static optical devices such as lenses, retarders, and reflectors have had a significant impact on the designs of many man-made optical technologies. However, while numerous adaptive and flexible optical mechanisms are found throughout the animal kingdom, highly desirable biomimetic copies of these remarkable smart systems remain, in many cases, a distant dream. Many aquatic animals have evolved highly efficient reflectors based on multilayer stacks of the crystallized nucleic acid base guanine. With exceptional levels of spectral and intensity control, these reflectors represent an interesting design pathway towards controllable micromirror structures. Here we show that individual guanine crystals, with dimensions of  $5 \mu\text{m} \times 20 \mu\text{m} \times 70 \text{ nm}$ , can be magnetically controlled to act as individual micromirrors. By applying magnetic fields of 500 mT, the reflectivity of these crystals can be switched off and on for the change in reflectivity. Overall, the use of guanine represents a novel design scheme for a highly efficient and controllable synthetic organic micromirror array.



## 1. INTRODUCTION

Biomineralization processes in living creatures can generate highly sophisticated microcrystal structures. For example, biogenic crystal complexes, which are made from either calcium carbonate or silica, have been found to show functional optical properties, including those of condensers, filters, and reflective structural color.<sup>1–9</sup> In addition to inorganic crystals, organic crystals can also act as optical devices in living creatures.<sup>9–14</sup>

Dynamic control of color and reflectivity in animal biophotonics far outstrip all current synthetic systems. For example, cephalopods provide astounding displays of color control using a hierarchical system of light-absorbing and light-reflecting chromatophores and iridophores.<sup>13,14</sup> Equally impressive in many regards are the similar transformative changes that occur in the multilayer and chromatophore-based optical structures of fish.<sup>9</sup> Certain fish use multilayer stacks of guanine crystals and cytoplasm that are equivalent to a distributed Bragg reflector on their scales and in a layer of their skin, called the argenteum.<sup>9–14</sup> Many species of fish also use similar multilayer reflectors in iridophores, such as the highly iridescent neon tetra (*Paracheirodon innesi*),<sup>12</sup> which controls the interference color of its blue dorsal flanks by dynamically selecting the wavelength of maximum reflection between ultraviolet (UV) and blue.

Such biological crystalline systems have provided numerous novel design solutions for synthetic optical devices,<sup>15</sup> and many new optical principles are still being discovered in nature.<sup>16–22</sup>

In the context of biological optics, the remarkable diversity of the available solutions for the same optical problem, which are examples of convergent evolution, still surprises researchers. One fundamental and key requirement for future man-made optical technologies is the efficient and dynamic control of light flow. For example, it is important to develop smaller microoptical controllers for both MEMS (micro-electro-mechanical systems) and microfluidic devices.<sup>23</sup> Several studies of silicon-based materials have successfully developed photonic structures that can actively control the velocity of light and its propagation and emission.<sup>24,25</sup> Similarly, periodic metamaterial structures can produce metamaterials which have new optical properties such as negative refractive indices.<sup>26–28</sup>

Guanine is found extensively in biological multilayer reflective structures<sup>10–14</sup> because it is energetically cheap to produce and because it exhibits one of the highest refractive indices found in any biological dielectric substance. The high refractive index contrast between guanine and cytoplasm leads to high efficiency in all thin (<20 layer) multilayer reflectors. Other interesting properties of guanine include optical biaxiality and high levels of intrinsic birefringence. Recent studies have shown that the relative directions of the optical axes are controlled in the different guanine crystal populations in the

Received: September 21, 2015

Revised: December 11, 2015

Published: December 12, 2015



reflector to reduce the effects of polarization by reflection.<sup>9,16</sup> In addition, crystallographic analyses have revealed that the biogenic crystals include both anhydrous and monohydrate crystals in the iridophore chambers of carp and goldfish.<sup>29–32</sup>

However, it is not simply the optical properties of guanine that are relevant to these dynamic optical structures. This study demonstrates that individual guanine crystals obtained from fish scales have anisotropic light scattering properties; the reflections from individual crystals can be controlled both by using their spatial orientation relative to the illumination direction and by changing the reflection from individual crystals using 500 millitesla (mT) magnetic fields.

## 2. EXPERIMENTAL SECTION

**2.1. Materials.** We used the fish scales of the goldfish, *Carassius auratus*, as the source of the guanine crystals. The collected scales to which skin tissues containing iridophores adhere were washed twice with distilled water, and by sticking the scales in a 12 mL centrifuge tube (Corning No. 430766) containing 1 mL of water using a plastic spatula (AsOne 1-9404-02), guanine crystals were released from the iridophores. After the water containing the guanine crystals was separated from the scales, the suspension was centrifuged at 1000 rpm for 3 s to exclude dust. The obtained supernatant was washed twice using distilled water through centrifugation twice at 3000 rpm for 6 min. For microscopic observation, the guanine crystals from the goldfish scales were contained in a closed thin glass chamber, where the guanine crystals sank and stayed statically at the bottom. The chamber used was a frame-seal incubation chamber (BIO-RAD SLF0201), which made a capacity of 25  $\mu$ L when the rubber frame was fixed to a glass plate (18 mm  $\times$  18 mm) and covered with another glass plate. By utilizing the rubber frame, a closed space with height of about 300  $\mu$ m was formed on a glass plate.

**2.2. Methods.** We developed two different methods for the evaluation of the light scattering anisotropies in the biogenic guanine crystals obtained from goldfish. By employing two independent methods, measurement reliability and reproducibility of experiment was validated.

In method-A (Figure 1A), the magnetic field generator was a resistive electromagnet (HDT-35-05TS, Hayama Ltd., Fukushima, Japan) with a maximum field of 500 mT in a 35 mm wide field exposure space between two magnetic poles. The sample chamber containing the guanine crystals was set in front of the charge-coupled device (CCD) microscope (VH-5000, Keyence Co. Ltd., Osaka, Japan) lens, which was set at the center between the poles. The lens (VH1001, Keyence) provided  $\times 1000$  magnification on its video screen. Numerical aperture (NA) of the lens cannot be supplied from the maker; however, we carried out the same kind of experiment by method-B which utilized a lens whose NA was 0.60 and checked the reproducibility of the obtained data. We arranged the light guides in the lens to direct two incident lights in a line, as shown in Figure 1A. In addition, the cap of the lens was rotated by 90°. As the outlets of light were fixed in two positions (center figure in Figure 1A), the rotation of the cap with the sample chamber was carried out without changing the incident light direction. In cases of magnetic field exposure experiments, the crystals were exposed to magnetic fields in the horizontal direction which was parallel to the incident light direction.

Figure 1B shows a schematic diagram of incident light in the sample chamber. The light was provided from a halogen lamp via an optical fiber. The utilized light guide in the lens (VH1001) directed the incident light to the horizontally placed sample chamber plane in an angle at 25°. This arrangement of incident light angle setting was followed by method-B (Figure 2). An additional light from a halogen lamp was supplied to the upper space of the sample chamber for taking a bright field image simultaneously.

In method-B (Figure 2A), the light scattering anisotropy measurement was carried out by using an inverted microscope (Olympus IX73) with a narrow sample stage (50 mm in width). The narrow stage

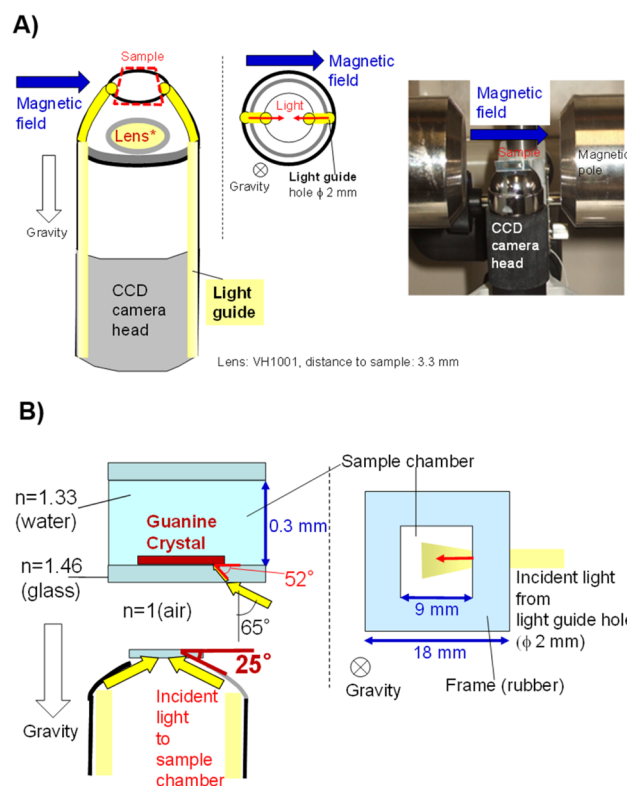


**Figure 1.** Experimental method-A for observing light scattering anisotropies in the biogenic guanine crystals. (A) Method-A with a fixed magnification lens and an electromagnet. The incident lights were in a line and provided by two light-guide fibers fixed at left- and right-handed sides of the lens (Keyence VH-1001, 1000 $\times$  magnification) on a CCD camera head (Keyence VH-5000). Magnetic field was applied parallel to the incident light direction. The right panel shows a photograph of the lens on the camera head between magnetic poles of an electromagnet (Hayama HDT-35-05TS). (B) Detailed schematic of the light incidence to sample. The light incidence angle was about 65°. The dark field illumination was provided by the light from a halogen lamp. In the case of observing the bright field image, an additional light source from a halogen lamp to the upper space of the sample chamber was introduced.

was designed to be set between the gap of magnet poles in the larger electromagnet (WS15-40-5K-MS, Hayama, Ltd., Fukushima, Japan) in method-B+. (Figure 2B). The utilized lens in that microscope was LUCPLFLN40XPH (NA = 0.60). The optical fiber was set below the narrow sample stage of the inverted microscope, and the incident light entered through a hole in the stage. The setting arrangement of incident light was carried out in the same way with method-A. In this schematic, the image of guanine crystal platelets with magnetic fields at 500 mT was obtained. The magnetic fields were switched on and off in 1 s using a voltage supplier in the experiments with the electromagnet (method-A and -B).

In order to investigate whether the observed guanine crystals were monoplates or stacks of plates, we carried out the measurements of the retardation along the z-axis of a platelet using digital hologram microscopy (DHM).<sup>9,33</sup> In brief, DHM is an interferometric-based microscopy technique that provides quantitative information on the retardation of light through a sample, permitting the measurement of optical path length. If the refractive index is known, then the technique provides an absolute measurement of the sample thickness with the accuracy of approximately 1 nm. Measurements were undertaken as described in ref 9, and using a refractive index value of 1.86 for the plane of the crystal, lengths of all three dimensions were measured for each crystal.

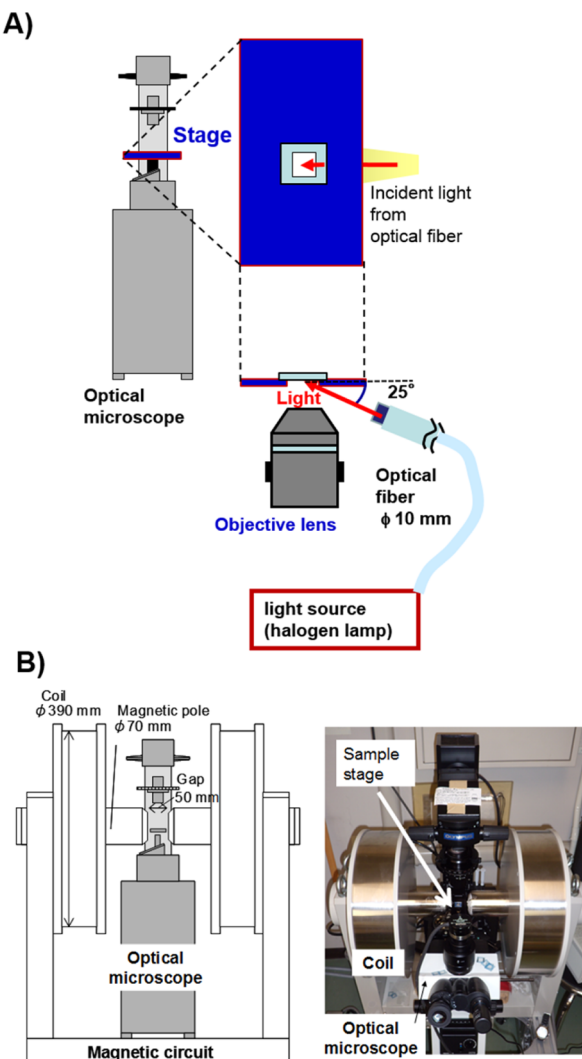


**Figure 2.** Experimental method-B and -B+ for observing light scattering anisotropies in the biogenic guanine crystals. (A) Method-B with a phase contrast microscope. (B) Method-B+ with a phase contrast microscope and an electromagnet (Hayama, WS15-40-5K-MS). An alteration was made on the stage of the microscope (Olympus IX73) to arrange the same kind of incident light with method-A.

### 3. RESULTS AND DISCUSSION

#### 3.1. Single Platelet Analyses of Light Reflection Anisotropy.

For initial characterization of the guanine crystals used in the experiment, we defined three orthogonal axes for each crystal (Figure 3A). For convenience, as a coordinate on the broadest surface ((102) plane<sup>31</sup>) of the crystal platelet, we defined the width and length of the broadest surface as the *x*-axis and the *y*-axis (*b*-axis of the crystal<sup>31</sup>), respectively. The typical sizes of the crystals in the length direction (*y*-axis) and in the width direction (*x*-axis) were 20–30 and 5  $\mu\text{m}$ , respectively.

As shown in Figure 3B and in the explanation of method-A (Figure 1B), the angle of the incident light with respect to the surface plane of the cover glass (vertical angle) was approximately 25°. The estimated angle with respect to the surface of a horizontally placed guanine crystal that was sank in water was approximately 52° (Figure 1B). Here, we make a distinction between two kinds of coordinates, in the platelet

(Figure 3A) and in the laboratory frame (Figure 3B). *X*, *Y*, and *Z* denote the axes of coordinate in the laboratory frame, and *x*, *y*, and *z* denote those defined in the body of a platelet. By rotating the cap of the lens (VH1001), the angle of incident light in *x*–*y* coordinate was changed by 0° to 90°, and it became possible to investigate how the reflection changes when a guanine crystal platelet rotated around its *z*-axis under an incident light exposure.

Figure 3C shows a single guanine crystal platelet that was illuminated in a sequence at angles of 0° (*L*(0)), 45° (*L*(45)), and 90° (*L*(90)) with respect to the *X*-axis. The results clearly show that the guanine crystal reversibly changed its brightness on its broadest surface between “bright” and “dark” when the incident light direction was changed by 90° in the *X*–*Y* plane of the space. This phenomenon was observed in many other platelets (Figure 3D). It was suggested that the light reflection in the broadest surface of the crystal platelet ((102) plane of crystal<sup>31</sup>) became bright and dark when an incident light directed perpendicular and parallel to *b*-axis, respectively.

To present a more quantitative evaluation, we counted the number of bright crystals when the incident light direction was set at *X*-axis (case of *L*(0)) and at *Y*-axis (case of *L*(90)), and plotted the number of bright crystals versus angle  $\varphi$ , respect to *Y*-axis (Figure 3E). The results show that the crystals tended to be bright when the incident light tended to direct perpendicular to the *y*-axis of the platelet in the *x*–*y* plane. An angle fluctuation of the axes within  $\pm 45^\circ$  did not change the brightness. The additional data on the change in reflection during the rotation of guanine crystal platelet around its *z*-axis are provide in the Supporting Information, Movie A.

Moreover, by utilizing method-B, it was found that the guanine crystal platelets exhibited a critical light reflection selectivity for the incident light to both long sides of the platelet (Figure 4). The crystal platelets utilized here were prealigned to one direction by a magnetic field exposure at 500 mT, and the direction to which the majority of the platelets align was set to the *Y*-axis of the laboratory frame. A careful comparison of the guanine crystal platelets under left-to-right and right-to-left illumination revealed that there were three kinds of platelets. Guanine crystals either reflected light that was incident from the right or the left. Or they showed no response.

Figure 4B shows the results of five measurements counting the platelets that became bright with illumination either from the right or left, or with no change (dark or bright for both illuminations). Among the total number of guanine crystal platelets from goldfish, about 46% of platelets showed the light reflection selectivity for the incident light to its width direction, while the other platelets did not change the reflection (Figure 4C).

We hypothesize that the mechanism of this phenomenon concerns rotation of platelet around its *y*-axis (*b*-axis of the crystal). The existence of the no-change platelets in Figure 4B,C indicated that half of the sampled platelets oriented parallel to the *X*–*Y* plane of the laboratory frame after they sank onto and adhered to the glass substrate. However, for the platelets that had an inclination of the *z*-axis, this tilt caused the reflection. Overall, the alignment of all of the platelets, as shown in Figure 4, revealed an equal division of reflecting platelets for two ways of incidence opposing to each other.

**3.2. Macroscopic Analyses of Light Reflection Anisotropy.** Macroscopic observations of multiple guanine crystals (Figure 5A–C) also showed the same effect, where only the guanine crystals that are orientated with their width (*x*-axis)

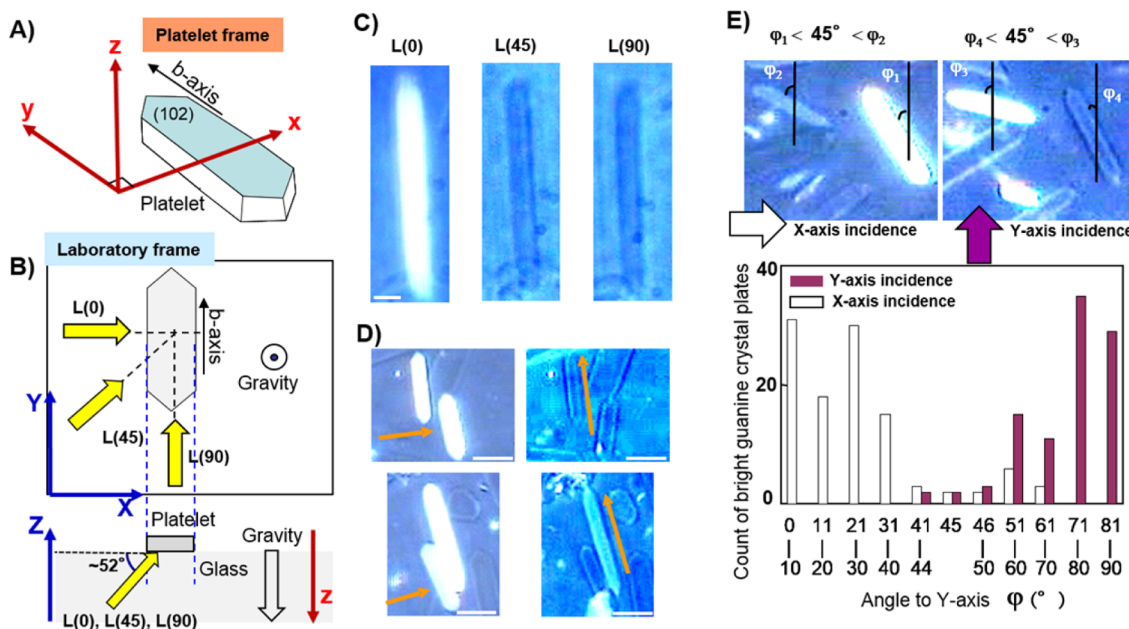


**Figure 3.** Effect of rotation around the  $z$ -axis of a guanine crystal platelet on the reflection in plate surface. The incident light direction was fixed (method-A, Figure 1A) in “Laboratory frame”,  $X-Y-Z$ , and the sample chamber in “platelet frame”,  $x-y-z$ , was rotated with the cap of the lens. (A) Diagram of coordinate in the broadest surface of a guanine crystal (coordinate in platelet frame,  $x-y-z$ ) and the directions of light incidence. (B) Schematic diagram of incident light to the guanine crystal platelet contacting on the bottom of the chamber (glass surface). Coordinate shows laboratory frame,  $X-Y-Z$ , except opposite directing  $z$  for the platelet frame. (C) Reflection only occurred for the incident light along the  $x$ -axis ( $L(0)$ ) and did not occur for  $L(45)$  and  $L(90)$ .  $L(\theta)$  denotes the direction of the light in the  $x-y$  plane, where  $\theta$  was the angle of incident light in the  $x-y$  plane. Bar,  $3 \mu\text{m}$ . (D) Another example of guanine crystal platelets showing bright reflections under light irradiation along the  $x$ -axis (left). Less bright guanine crystal platelets under light irradiation along the  $y$ -axis (right). Bar,  $10 \mu\text{m}$ . (E) Analysis of reflection change when a guanine crystal platelet rotates around the  $z$ -axis under incident light to the  $X$ -axis and  $Y$ -axis in the laboratory frame.  $\varphi$  is the angle between the reference axis and the direction of the  $y$ -axis in each platelet. The histogram shows the dependence of the number of bright platelets on the angle between the reference axis and the  $y$ -axis of the individual platelet, where  $n = 98$  for  $Y$ -axis incidence and  $n = 111$  for  $X$ -axis incidence.

parallel to the direction of incident light were reflective. The crystal platelets in Figure 5A were exposed to light from all directions in the  $X-Y$  plane, so a random orientation of bright platelets appeared. Reflections only occurred from the platelets where the  $x$ -axis was parallel to the illumination direction, for example illumination from the bottom (Figure 5B) or right (Figure 5C) in the image. The images in Figure 5B,C also indicate that a fluctuation of rotation around the  $z$ -axis of platelet by  $45^\circ$  maintained the reflection.

To confirm that this effect was not simply a consequence of an artifact in the light source positioning, we prealigned the individual guanine crystals by applying magnetic fields parallel to the sample chamber and then horizontally rotating the chamber around  $Z$ -axis while the direction of incident light remained fixed (Figure 5D–G). Figure 5D shows the orientation of the platelets after an exposure of  $500 \text{ mT}$ . The  $y$ -axis ( $b$ -axis) of most of the platelets can be seen to be at an angle of  $0-40^\circ$  to the  $Y$ -axis and, as a result, show little reflection. The count of bright platelets gradually increased while rotating the sample chamber as the  $X$ -axes of the guanine crystals lined up with the direction of the incident light (Figure 5G).

Overall these data indicated that the reflectivity of the crystals changed as they rotated around either the  $z$ -axis or the  $y$ -axis. Any effect of the rotation around the  $x$ -axis was not detectable because the moment of inertia of platelet was too large in that direction.

### 3.3. Magnetic Control of Light Reflection in Guanine Crystal Platelets.

Finally, we discovered a way to switch the guanine reflectivity on and off by using magnetic fields. The

“reflection-on” state was created with the incident light along the  $x$ -axis of platelet (Figure 6A,B,E), and, keeping everything else unchanged, the “reflection-off” state was induced by switching on the magnetic field (Figure 6C,D,F,G). The reflective platelets (marked by a white circle in Figure 6A) exhibited the same brightness whether the bright field illumination from the microscope was present or not (Figure 6B). When a magnetic field of  $500 \text{ mT}$  (Figure 6C,D) was applied, the marked platelets became less bright and disappeared in the absence of bright field illumination. Clearly some platelets rotated around the  $Z$ -axis; however, the rotation around the  $Z$ -axis did not affect the brightness until the rotation exceeded  $45^\circ$ .

The images in Figure 6E,F show other examples. More than 20 guanine crystal platelets show a bright reflection (Figure 6E) until a  $500 \text{ mT}$  magnetic field (Figure 6F) is applied and then the reflection is inhibited. For the real-time observation of the phenomenon, see the Supporting Information, Movie B.

In addition to the immediate change in the reflection caused by magnetic fields, a slow rotation of platelets occurred (over approximately 4.5 min), orienting the  $y$ -axis of the platelet to the  $Y$ -axis (Figure 6F,G). If all of the platelets aligned to the applied magnetic fields, the platelets directing to the incident light should be less bright even right after the magnetic field is off. However, in Figure 6H, three platelets turned to bright immediately after the magnetic field was turned off. During the magnetic field on, two of them did not rotate due to a confliction and their  $x$ -axis remained in parallel to the incident light. One of them (smaller bright platelets in Figure 6H) obviously caused disorientation after the diamagnetic torque

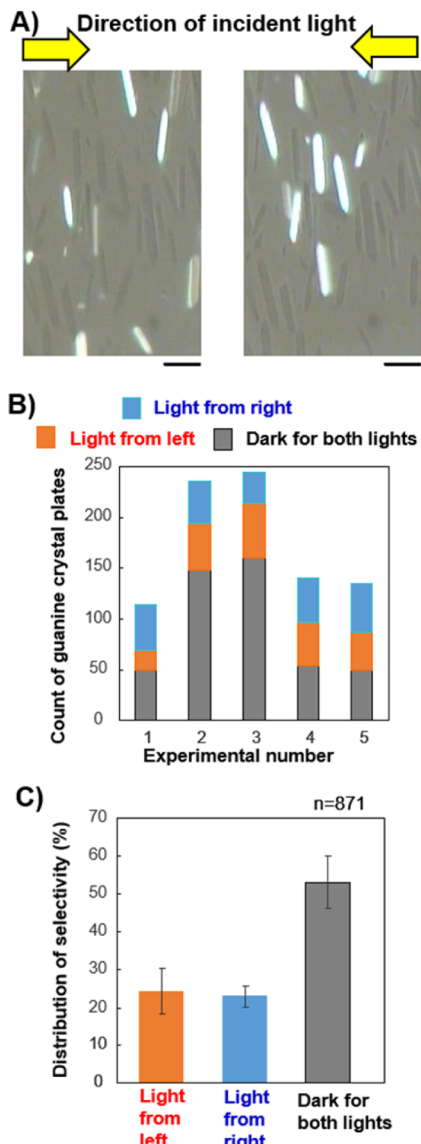


**Figure 4.** Effect of changing the incident light direction around the  $y$ -axis of a guanine crystal platelet on the reflection in the platelet surface. (A) Photographs of guanine crystal platelets showing reflection for two ways of incident light (from left,  $-Y$  and from right,  $+Y$ ). Bar, 10  $\mu\text{m}$ . (B) Examples of counts in three kinds of crystal platelets, bright either under from-left or from-right incidence, and continuously dark. (C) Statistical presentation of the light reflection selectivity on the broadest surface ((102) plane) of guanine crystal platelets of goldfish (number of the platelet counts = 871).

force fixing the platelet disappeared. These reasons can explain the recovery of reflection in the postexposure of magnetic fields. It is notable that the observed fast magnetic light switching behavior (Figure 6A–F) was generated independently of the slow magnetic orientation (Figure 6G).

When in solution, guanine crystal platelets show dynamic motion that creates a flickering of the reflected light. This is believed to be because of Brownian motion; the guanine platelet showed frequent tilting around the  $x$ -axis while showing less tilting around the  $y$ -axis of the platelet. The freedom of rotation around the  $x$ -axis is sufficient to explain the observed light switching off by magnetic fields (Figure 6). By comparing the projected dimensions of crystal platelets in Figure 6F with Figure 6E, we see a change in projection of the width of the

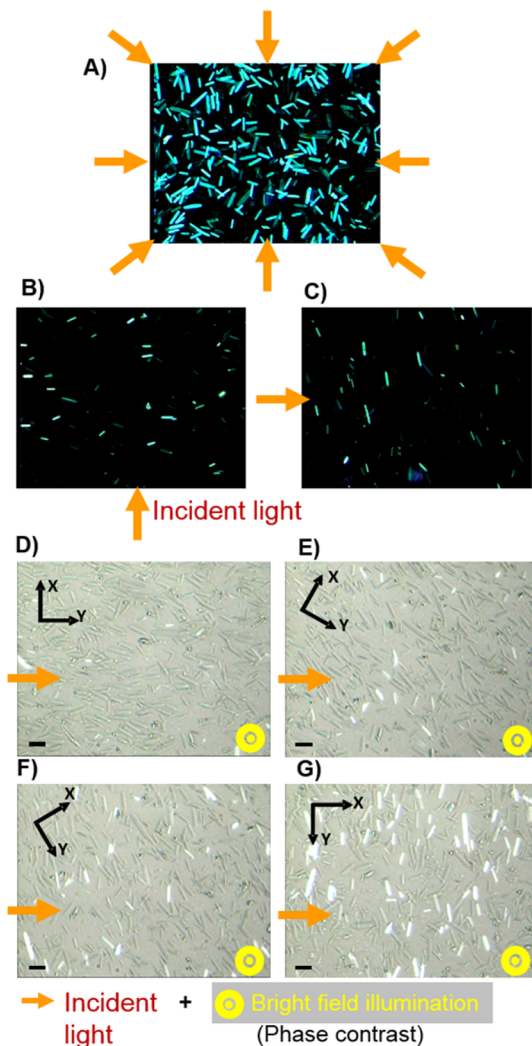


**Figure 5.** Macroscopic observation of guanine crystal platelets on a glass plate. (A) Incident light surrounding the platelets on all sides. (B) Single light incidence direction from bottom to top in the photograph. (C) Light incidence from left to right. (D) Crystal platelets were prealigned on a glass plate by external magnetic fields of 500 mT, and the direction of the  $y$ -axis of the aligned crystal platelets (the  $b$ -axis of the anhydrous guanine crystal) towards the incident light from left to right created less bright conditions. (E, F) Rotation of the sample chamber increased the number of bright guanine crystal platelets. (G) Maximum brightness was obtained for the crystal platelets when the  $y$ -axis of the aligned platelets was vertical to the incident light. The bar represents 10  $\mu\text{m}$ . The photographs were taken with both bright field and dark field illumination (incident light).

platelet of approximately 200 nm, which suggests the platelet magnetically rotated by  $16^\circ$  at least.

Finally to conclusively discover whether the observed crystals in the experiments were single crystals and not stacked groups, we measured the thicknesses directly using digital hologram microscopy. As shown in Figure 7A,B and Table 1, the guanine platelets had an averaged thickness of  $65.1 \pm 4.1$  nm which varied by 10–20 nm across the width of the crystal whose average was  $5150 \pm 950$  nm. The estimated slope angle was  $0.1\text{--}0.2^\circ$ , which is too small to reflect the incident light at the angle measured. So we can conclude that as the orientation of the illumination changes relative to the  $x$ -axis of the guanine crystal, the associated changes in the reflectivity are due to the inclination of the platelet itself.

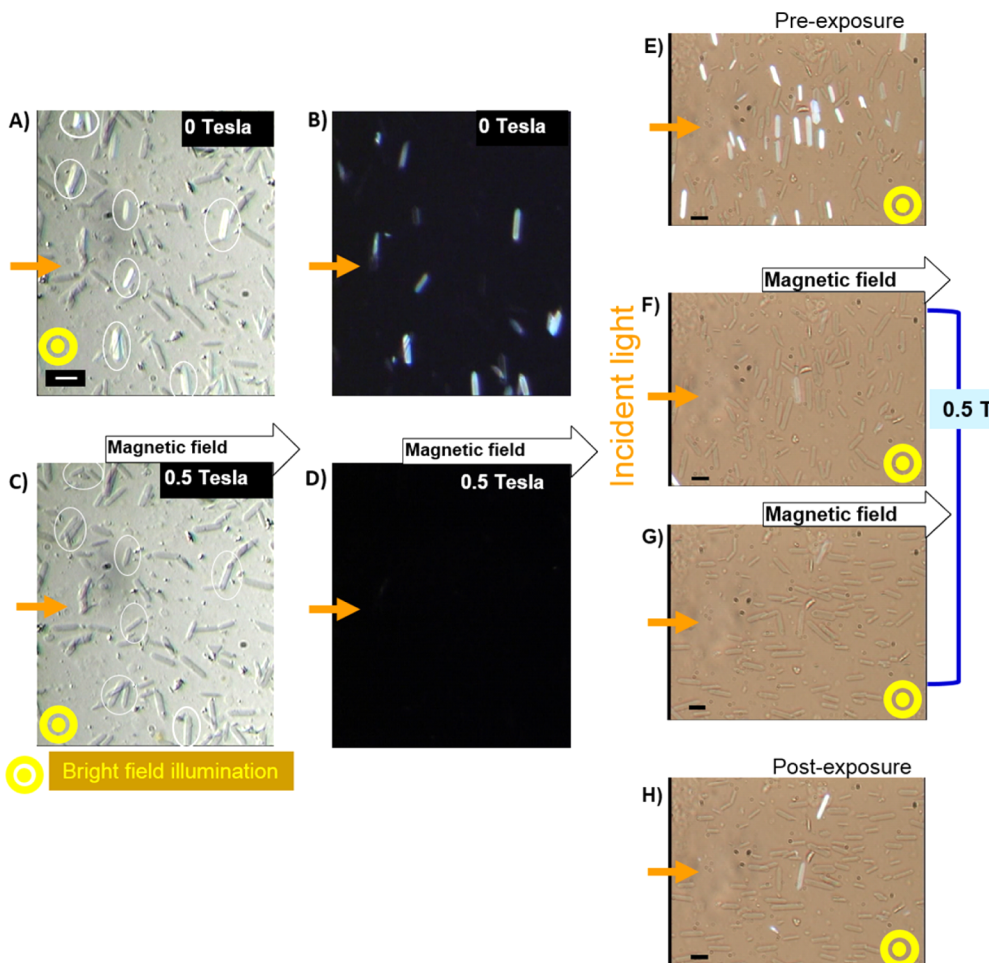


**Figure 6.** Magnetically induced switching of light reflection in guanine crystal platelets. The incident light and magnetic fields were provided along the X-axis of the laboratory frame. First example without magnetic field exposure (A, B) and with magnetic fields at 500 mT (C, D). (A) Bright field illumination image of guanine crystals accompanying an incident light (orange arrow) in the left-to-right direction. The bright platelet is marked by a circle. (B) Same crystals with the incident light alone. (C) Bright field image accompanying the applied incident light and magnetic fields. (D) Same crystals with incident light and 500 mT magnetic fields. Second example: (E) before magnetic field exposure, (F) immediately after the 500 mT magnetic field was applied from left to right (in X-axis of laboratory frame; the light reflection towards the z-axis in the guanine crystals became less bright at 500 mT), (G) 4.5 min after the 500 mT magnetic field exposure began (the y-axes of the crystals became parallel with the applied magnetic fields), and (H) immediately after the magnetic field was turned off. The bar represents 10  $\mu$ m.

To demonstrate that this proposed mechanism is feasible, we are able to verify that the diamagnetic energy is greater than the thermal fluctuation energy of the crystals in water. Previously, the magnetic energy in a diamagnetic guanine crystal has been estimated by considering the diamagnetic anisotropy<sup>34</sup> of a guanine molecule. By comparing guanine with benzene, whose diamagnetic anisotropy  $\Delta K$  was reported to be  $49.2 \times 10^{-12} \text{ m}^3 \text{ mol}^{-1}$ <sup>35</sup>, we estimated the  $\Delta K$  of guanine as  $63.3 \times 10^{-12} \text{ m}^3 \text{ mol}^{-1}$ . Using values of the density ( $\rho = 2.2 \text{ g cm}^{-3}$ ) and molar mass ( $M = 151.13 \text{ g mol}^{-1}$ ), the volumetric anisotropy in the magnetic susceptibility of guanine was determined to be  $\Delta \chi = \Delta K/M = 9.2 \times 10^{-1} \text{ m}^{-3} \text{ mol}^{-1}$ . From this, the diamagnetic anisotropic energy can be determined using

$$\Delta E_{\text{anisotropy}} = -\Delta \chi V \frac{B^2}{2\mu_0} \quad (1)$$

where  $B$  is magnetic field;  $\mu_0$  is the magnetic permeability of vacuum, and  $V$  is the volume of the object. Because the rings of guanine molecule are in parallel to the broadest surface ((102) plane) of the crystal platelet,<sup>31</sup> we employed this  $\Delta \chi$  for the

energy estimation. The volume of the object was obtained by the size of a guanine crystal platelet,  $20,000 \text{ nm} \times 5,000 \text{ nm} \times 70 \text{ nm}$ . The obtained diamagnetic anisotropic energy was  $8 \times 10^{-18} \text{ J}$ . When viewed in the context of thermal energy  $kT = 4.14 \times 10^{-21} \text{ J}$  ( $k$  is Boltzmann constant, and  $T$  is temperature), the energy for the diamagnetic rotation of a guanine crystal platelet is approximately 1900 times larger than the thermal fluctuations disturbing the magnetic orientation of the object. The rotation around  $y$ -axis ( $b$ -axis of the crystal) occurred rapidly because the  $\Delta \chi$ , anisotropy of diamagnetic susceptibility, between  $z$ -axis and  $y$ -axis was maximum under the external magnetic field. The  $\Delta \chi$  between  $y$ -axis and  $x$ -axis was relatively small, so the rotation around the  $z$ -axis by  $90^\circ$  needed about 5 min.

#### 4. CONCLUSIONS

In this study, we found that biogenic guanine crystal platelets, obtained from goldfish, have a specific selectivity for light reflection from their broadest surfaces. In addition, light reflection in the guanine crystal platelets could be switched off magnetically with a small tilting of the crystal. Under dark

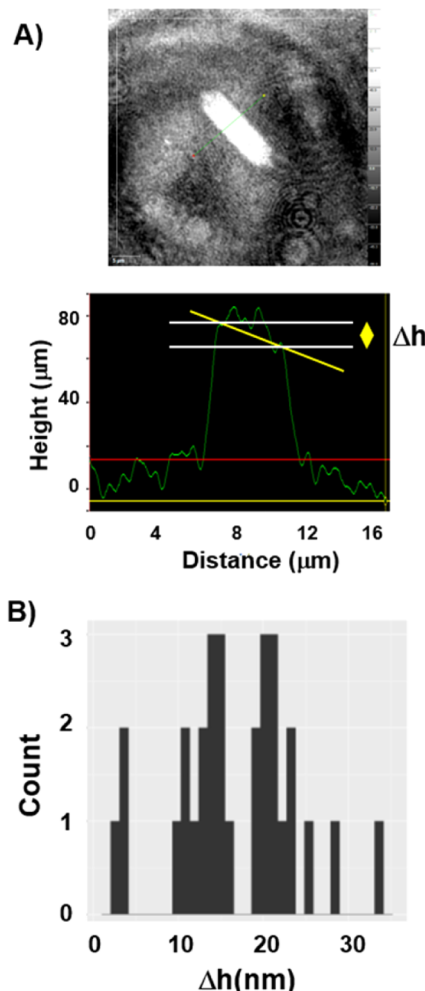


**Figure 7.** Measurement of thickness of goldfish's guanine crystals from their scales. (A) Quantitative phase image and calculated height of a guanine crystal platelet obtained by the digital hologram microscopy. (B) Histogram of  $\Delta h$ , inclination in the broadest surface (102 plane) of guanine crystal platelet, i.e., the difference of height between start and end points along the width direction ( $x$ -axis in Figure 3A).

**Table 1. Width and Thickness of Goldfish Guanine Crystal Platelets Measured by a Digital Holographic Microscopy ( $n = 10$ )**

width (mean $\pm$ SD)	thickness (mean $\pm$ SD)
$5.15 \pm 0.95 \mu\text{m}$	$65.1 \pm 4.1 \text{ nm}$

field illumination, the biogenic crystal platelets showed strong light reflection on their broadest planes by reflecting light with an angle of incidence of  $\sim 38^\circ$ ; however, the strong reflection only occurred when the angle of incidence was directed perpendicular to the length of the crystal platelet. Moreover, immediately after the application of the external magnetic field at  $\sim 500 \text{ mT}$ , reflections from the crystals switched off rapidly. As a general conclusion, this mechanism of rotation provides a novel method for the rapid control of micro-mirror plates over small angular ranges. Such control has implications for future efficient biomedical optical MEMS devices in an aqueous media. Also these methods may provide a new analysis technique for microscopic and real-time measurement of the color and reflectivity in animal biophotonic structures.

## ASSOCIATED CONTENT

### Supporting Information

The Supporting Information is available free of charge on the ACS Publications website at DOI: [10.1021/acs.langmuir.Sb03522](https://doi.org/10.1021/acs.langmuir.Sb03522).

Detailed explanations for the light reflection change in guanine crystal platelets during the magnetic field exposure and the rotation around  $z$ -axis ([PDF](#))

Movie A rotation showing rotation of guanine crystal platelets around  $Z$ -axis while maintaining the incident light direction ([AVI](#))

Movie B magnetic field showing light reflection change in guanine crystal platelets under 500 mT magnetic fields ([AVI](#))

## AUTHOR INFORMATION

### Corresponding Author

\*E-mail: [iwasaka@hiroshima-u.ac.jp](mailto:iwasaka@hiroshima-u.ac.jp).

### Notes

The authors declare no competing financial interest.

## ACKNOWLEDGMENTS

This study was supported by JST, PRESTO, "Creation of Basic Technology for Improved Bioenergy Production through Functional Analysis and Regulation of Algae and Other Aquatic Microorganisms."

## REFERENCES

- Song, Y. M.; Xie, Y.; Malyarchuk, V.; Xiao, J.; Jung, I.; Choi, K.-J.; Liu, Z.; Park, H.; Lu, C.; Kim, R.-H.; Li, R.; Crozier, K. B.; Huang, Y.; Rogers, J. A. Digital cameras with designs inspired by the arthropod eye. *Nature* **2013**, *497*, 95–99.
- Lee, K.; Wagermaier, W.; Masic, A.; Kommareddy, K. P.; Bennet, M.; Manjubala, I.; Lee, S.-W.; Park, S. B.; Cölfen, H.; Fratzl, P. Self-assembly of amorphous calcium carbonate microlens arrays. *Nat. Commun.* **2012**, *3*, 725.
- Aizenberg, J.; Tkachenko, A.; Weiner, S.; Addadi, L.; Hendler, G. Calcitic microlenses as part of the photoreceptor system in brittlestars. *Nature* **2001**, *412*, 819–822.
- Sundar, V. C.; Yablon, A. D.; Grazul, J. L.; Ilan, M.; Aizenberg, J. Fibre-optical features of a glass sponge—some superior technological secrets have come to light from a deep-sea organism. *Nature* **2003**, *424*, 899–900.
- Roberts, N. W.; Chiou, T. H.; Marshall, N. J.; Cronin, T. W. A biological quarter-wave retarder with excellent achromaticity in the visible wavelength region. *Nat. Photonics* **2009**, *3*, 641–644.
- Jen, Y.-J.; Lakhtakia, A.; Yu, C.-W.; Lin, C.-F.; Lin, M.-J.; Wang, S.-H.; Lai, J.-R. Bio-inspired Achromatic Waveplates for Visible Light. *Nat. Commun.* **2011**, *2*, 363.
- Angel, J. R. P. Lobster eyes as X-ray telescopes. *Astrophys. J.* **1979**, *233*, 364–373.
- Vukusic, P.; Sambles, J. R.; Lawrence, C. R.; Wootton, R. J. Structural colour: Now you see it — now you don't. *Nature* **2001**, *410*, 36.
- Jordan, T. M.; Partridge, J. C.; Roberts, N. W. Non-polarizing broadband multilayer reflectors in fish. *Nat. Photonics* **2012**, *6*, 759–763.
- Denton, E. J. Review Lecture: On the organization of reflecting surfaces in some marine animals. *Philos. Trans. R. Soc., B* **1970**, *258*, 285–313.
- Herring, P. J. Reflective systems in aquatic animals. *Comp. Biochem. Physiol., Part A: Physiol.* **1994**, *109*, 513–546.
- Lythgoe, J. N.; Shand, J. Changes in spectral reflexions from the iridophores of the Neon tetra. *J. Physiol.* **1982**, *325*, 23–34.

- (13) Denton, E. J.; Land, M. F. Mechanism of Reflexion in Silvery Layers of Fish and Cephalopods. *Proc. R. Soc. London, Ser. B* **1971**, *178*, 43–61.
- (14) Hanlon, R. T. The functional organization of chromatophores and iridescent cells in the body patterning of *Loligo plei* (Cephalopoda: Myopsida). *Malacologia* **1982**, *23*, 89–119.
- (15) Douglas, T. A. Bright Bio-Inspired Future. *Science* **2003**, *299*, 1192–1193.
- (16) Jordan, T. M.; Partridge, J. C.; Roberts, N. W. Suppression of Brewster delocalization anomalies in an alternating isotropic-birefringent random layered medium. *Phys. Rev. B: Condens. Matter Mater. Phys.* **2013**, *88*, 041105.
- (17) Debord, J. D.; Eustis, S.; Debord, S. B.; Lofye, M. T.; Lyon, L. A. Color-Tunable Colloidal Crystals from Soft Hydrogel Nanoparticles. *Adv. Mater.* **2002**, *14*, 658–662.
- (18) Zhao, Y.; Xie, Z.; Gu, H.; Zhu, C.; Gu, Z. Bio-inspired variable structural color materials. *Chem. Soc. Rev.* **2012**, *41*, 3297–3317.
- (19) Xu, J.; Guo, Z. J. Biomimetic photonic materials with tunable structural colors. *J. Colloid Interface Sci.* **2013**, *406*, 1–17.
- (20) Kolle, M.; Lethbridge, A.; Kreysing, M.; Baumberg, J. J.; Aizenberg, J.; Vukusic, P. Bio-Inspired Band-Gap Tunable Elastic Optical Multilayer Fibers. *Adv. Mater.* **2013**, *25*, 2239–2245.
- (21) Bai, L.; Xie, Z.; Wang, W.; Yuan, C.; Zhao, Y.; Mu, Z.; Zhong, Q.; Gu, Z. Bio-Inspired Vapor-Responsive Colloidal Photonic Crystal Patterns by Inkjet Printing. *ACS Nano* **2014**, *8*, 11094–11100.
- (22) Lapidot, S.; Meirovitch, S.; Sharon, S.; Heyman, A.; Kaplan, D. L.; Shoseyov, O. Clues for biomimetics from natural composite materials. *Nanomedicine* **2012**, *7*, 1409–1423.
- (23) Psaltis, D.; Quake, S. R.; Yang, C. Developing optofluidic technology through the fusion of microfluidics and optics. *Nature* **2006**, *442*, 381–386.
- (24) Noda, S.; Chutinan, A.; Imada, M. Trapping and emission of photons by a single defect in a photonic bandgap structure. *Nature* **2000**, *407*, 608–610.
- (25) John, S. Light control at will. *Nature* **2009**, *460*, 337.
- (26) Kawata, S.; Inouye, Y.; Verma, P. Plasmonics for near-field nano-imaging and superlensing. *Nat. Photonics* **2009**, *3*, 388–394.
- (27) Tanaka, T.; Ishikawa, A.; Kawata, S. Unattenuated light transmission through the interface between two materials with different indices of refraction using magnetic metamaterials. *Phys. Rev. B: Condens. Matter Mater. Phys.* **2006**, *73*, 125423.
- (28) Pendry, J. B.; Schurig, D.; Smith, D. R. Controlling Electromagnetic Fields. *Science* **2006**, *312*, 1780–1782.
- (29) Guille, K.; Clegg, W. Anhydrous guanine: A synchrotron study. *Acta Crystallogr., Sect. C: Cryst. Struct. Commun.* **2006**, *62*, o515–o517.
- (30) Thewalt, U.; Bugg, C. E.; Marsh, R. E. The crystal structure of guanine monohydrate. *Acta Crystallogr., Sect. B: Struct. Crystallogr. Cryst. Chem.* **1971**, *27*, 2358–2363.
- (31) Levy-Lior, A.; Pokroy, B.; Levavi-Sivan, B.; Leiserowitz, L.; Weiner, S.; Addadi, L. Biogenic Guanine Crystals from the Skin of Fish May Be Designed to Enhance Light Reflectance. *Cryst. Growth Des.* **2008**, *8*, 507–511.
- (32) Iwasaka, M.; Mizukawa, Y. Light Reflection Control in Biogenic Micro-Mirror by Diamagnetic Orientation. *Langmuir* **2013**, *29*, 4328–4334.
- (33) Kim, M. K. Principles and techniques of digital holographic microscopy. *J. Photonics Energy* **2010**, *1*, 018005.
- (34) Pauling, L. The Diamagnetic Anisotropy of Aromatic Molecules. *J. Chem. Phys.* **1936**, *4*, 673–677.
- (35) Pauling, L. Diamagnetic anisotropy of the peptide group. *Proc. Natl. Acad. Sci. U. S. A.* **1979**, *76*, 2293–2294.